

# **Stochastic Gravitational-Wave Background**

**Guo Chin Liu**

**Department of Physics, Tamkang University**

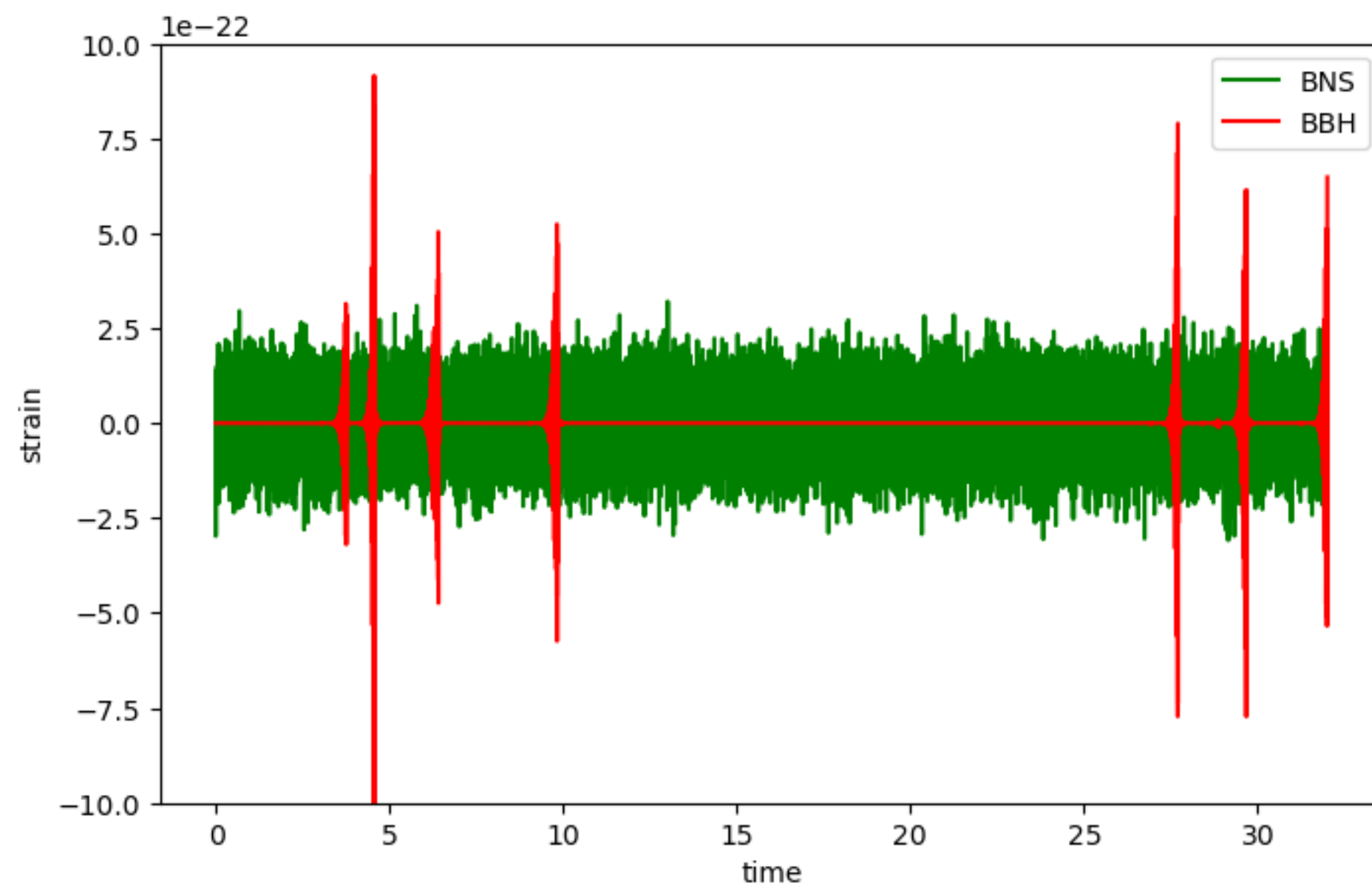
**Open Data Workshop, April 18-20, 2024**

# Stochastic Background

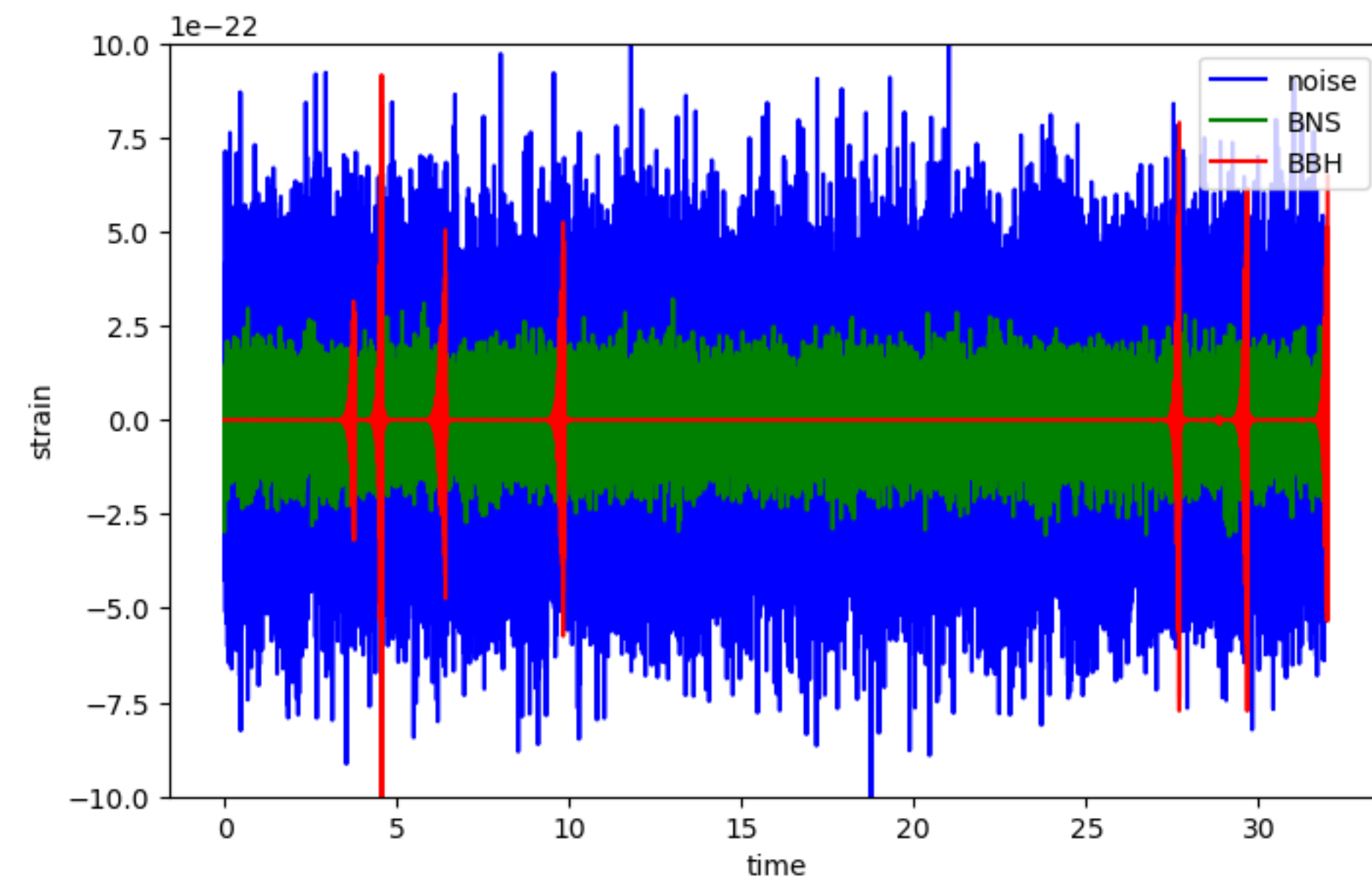
## Superposition of many faint, unsolved gravitational-wave signals

- Cosmological sources: phase transition, inflation, cosmic string...
- Astrophysics sources: CBC, Core collapse supernovae, rapidly rotating NS...

GW signals



noise+GW signals



We study the statistical properties of the background

# Plane wave expansion of metric perturbations

$$h_{ab}(t, \vec{x}) = \int_{-\infty}^{\infty} df \int d^2\Omega_{\hat{n}} \sum_{A=+, \times} h_A(f, \hat{n}) e_{ab}^A(\hat{n}) e^{i2\pi f(t + \hat{n} \cdot \vec{x}/c)}$$

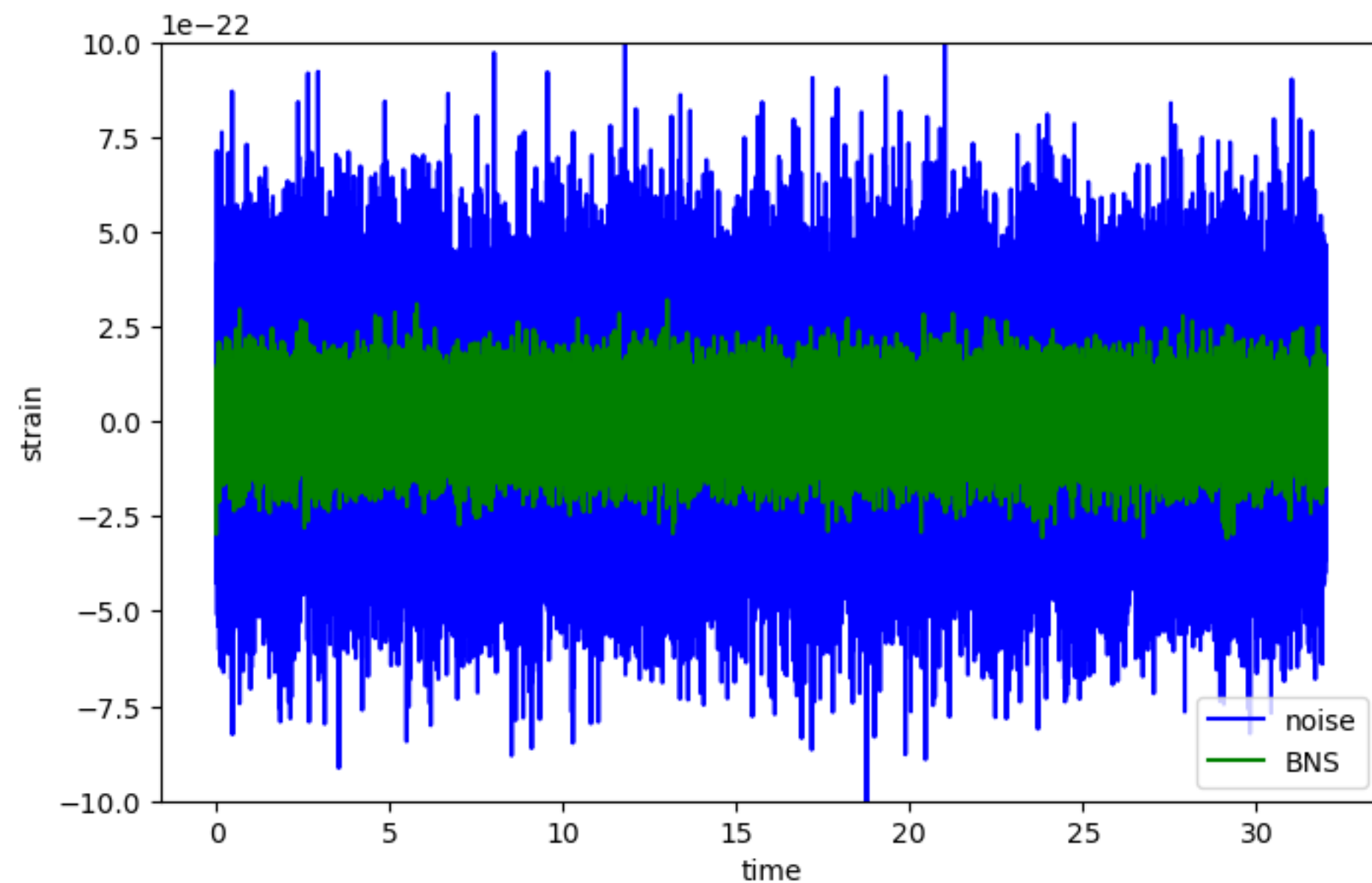
We can investigate the statistical properties of SGWB by measuring

$\langle h_{ab}(t, \vec{x}) \rangle$		$\langle h_A(f, \hat{n}) \rangle$
$\langle h_{ab}(t, \vec{x}) h_{cd}(t', \vec{x}') \rangle$		$\langle h_A(f, \hat{n}) h_{A'}(f', \hat{n}') \rangle$
$\langle h_{ab}(t, \vec{x}) h_{cd}(t', \vec{x}') h_{ef}(t'', \vec{x}'') \rangle$		$\langle h_A(f, \hat{n}) h_{A'}(f', \hat{n}') h_{A''}(f'', \hat{n}'') \rangle$

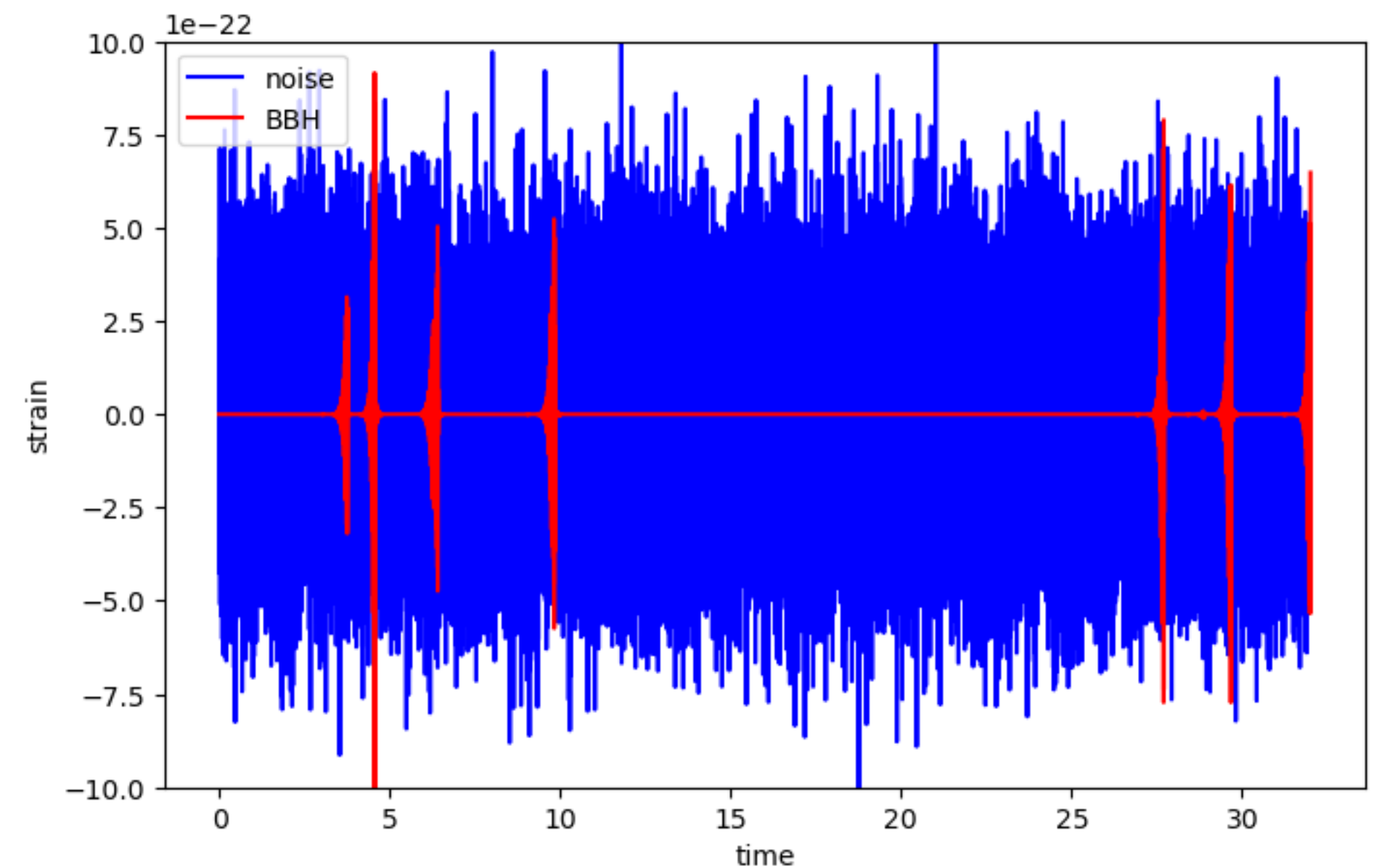
# In the previous studies of SGWB, we assumed:

- The GW signals (and noise) are stationary Gaussian
- The GW signals are unpolarized
- Noise in different detectors is uncorrelated

The rate of signals is large enough, the signal will be stationary Gaussian



The rate of signals is small, the signals will be non-stationary and non-Gaussian



**The Gaussian backgrounds are fully characterized by the quadratic expectation value. For non-Gaussian backgrounds, higher order moments are needed.**

# Gaussian Background

## Quadratic expectation values

For a stationary, Gaussian, unpolarized and isotropic background:

$$\left\langle h_A(f, \hat{n}) h_{A'}^*(f', \hat{n}') \right\rangle = \frac{1}{16\pi} S_h(f) \delta(f - f') \delta_{AA'} \delta^2(\hat{n}, \hat{n}')$$

$S_h(f)$ : one-sided GW strain power spectral density function

$$S_h(f) = \frac{3H_0^2}{2\pi^2} \frac{\Omega_{GW}(f)}{f^3}$$

$$\Omega_{GW}(f) \equiv \frac{1}{\rho_c} \frac{d\rho_{GW}}{d \ln f}$$

For a stationary, Gaussian, unpolarized and anisotropic background:

$$\left\langle h_A(f, \hat{n}) h_{A'}^*(f', \hat{n}') \right\rangle = \frac{1}{4} \mathcal{P}(f, \hat{n}) \delta(f - f') \delta_{AA'}$$

$\mathcal{P}(f, \hat{n})$ : spatial distribution of GW power on the sky

Fractional energy density spectrum in GW

# What we try to learn from SGWB?

- Energy level of the isotropic GW background
  - Tensor and non-tensorial polarization background
  - Implications on cosmological and astrophysical models
- Anisotropic GW background
  - Any (detectable) GW signals from particular direction and/or at particular frequency (for example: due to the kinetic dipole or distribution of matter in local universe)
- Intermittent background
  - Learn the duty cycle and energy density contributed by BBH mergers.



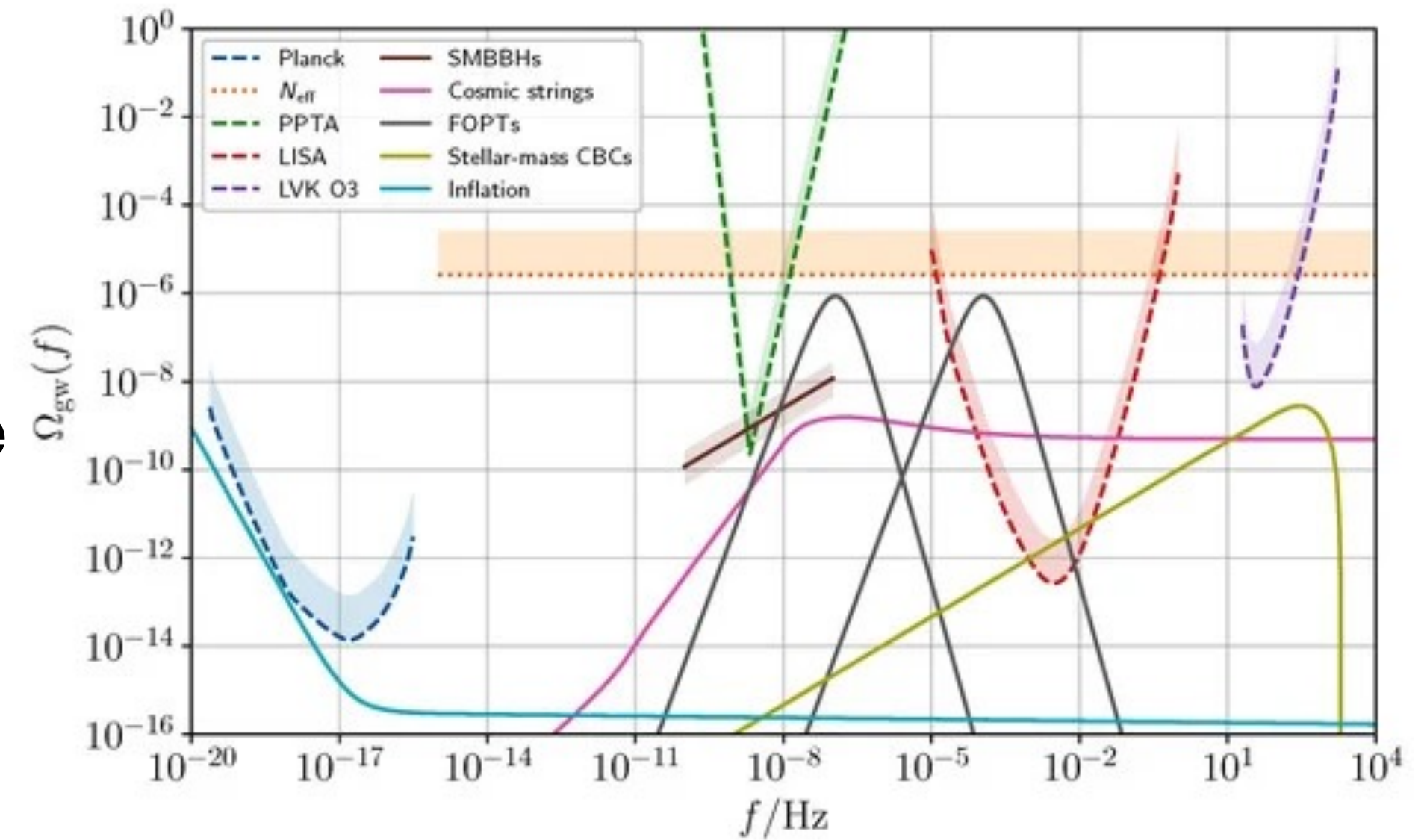
# $\Omega_{GW}(f)$

$$\Omega_{GW}(f) = \frac{1}{\rho_c} \int_0^\infty dz \frac{N(z)}{1+z} \left[ f_r \frac{dE_{GW}}{df_r} \right]_{f_r=f(1+z)}$$

$N(z)$ : number of GW emitters as function of  $z$

$f_r$ : emission frequency in the rest frame of the source

$\frac{dE_{GW}}{df_r}$ : spectral energy density of a specific source



Rennin et al. 2022

The spectral dependence of a specific source is often reduced to a power law

$$\Omega_{GW}(f) = \Omega_{GW}(f_{\text{ref}}) \left( \frac{f}{f_{\text{ref}}} \right)^\alpha$$

# Search Gaussian SGWB

## SGWB contributes extra power on our data.

Problem: Distinguishing GW signals from noise in individual detectors is challenging.

Solution: Cross-Correlation of the data from two detectors can suppress the uncorrelated noise

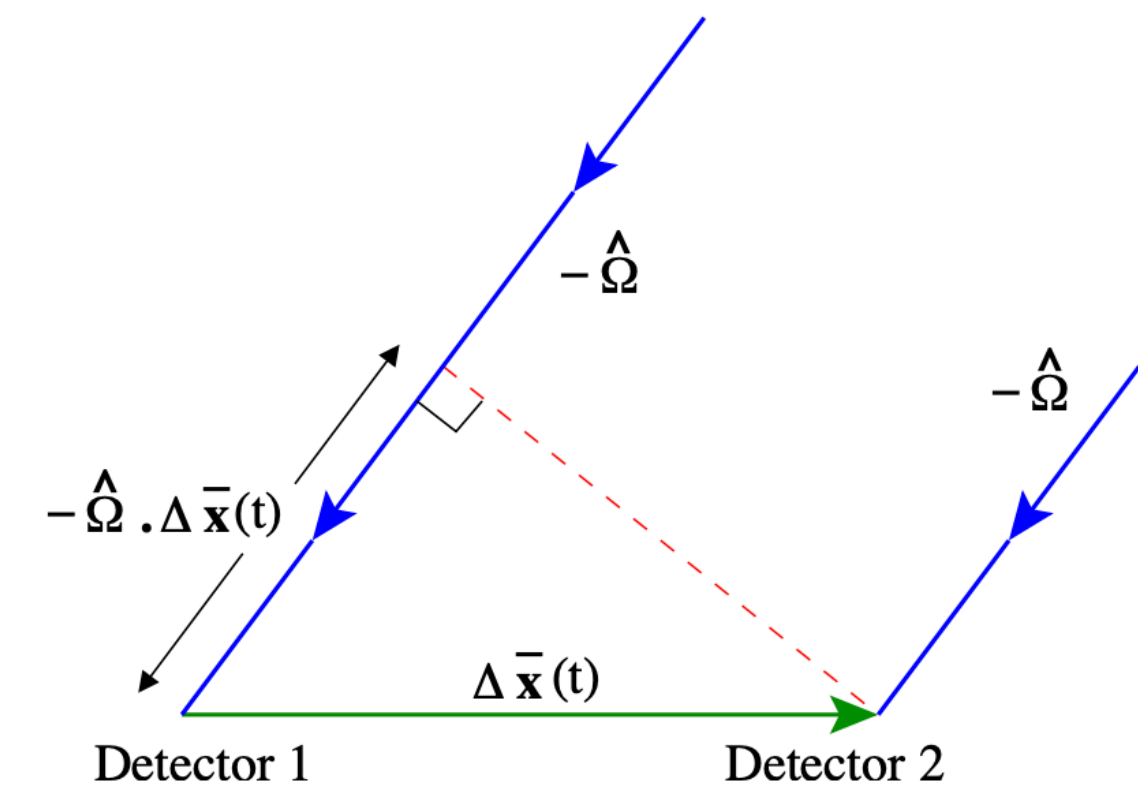
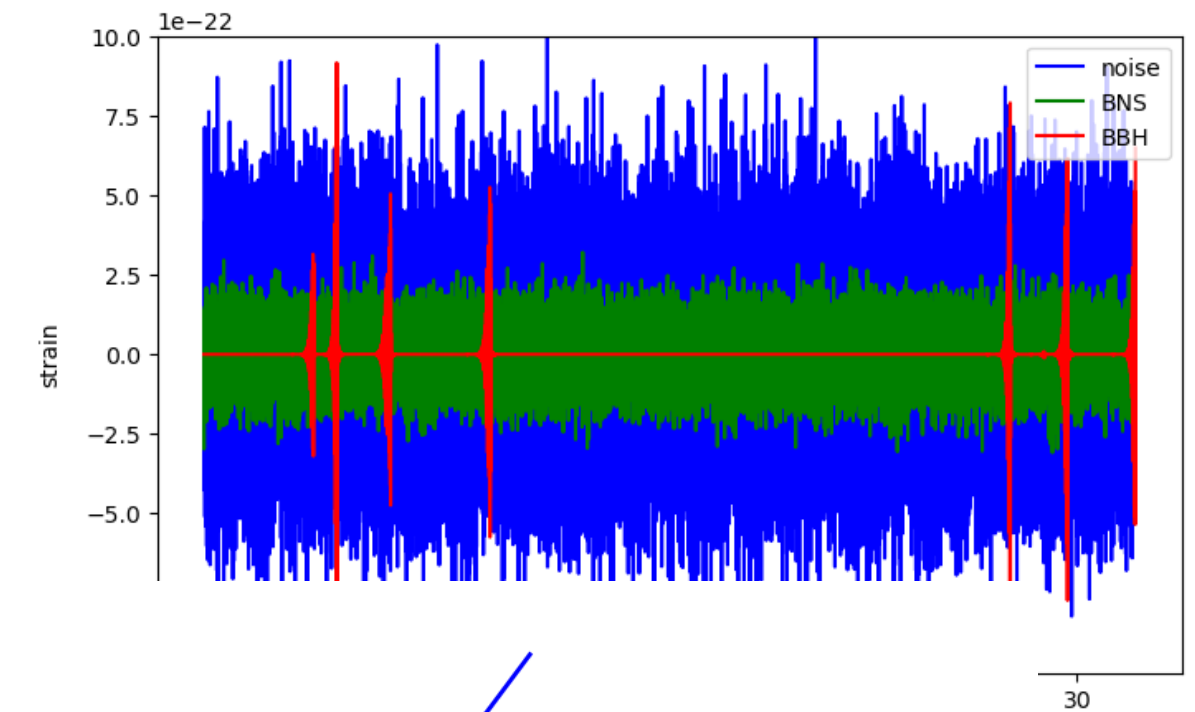
$$\text{Output in detector I : } \tilde{h}_I(f) = \int d^2\Omega_{\hat{n}} \sum_A R_I^A(f, \hat{n}) h_A(f, \hat{n})$$

$$\text{Detector response } R_I^A(f, \hat{n}) = \frac{1}{2}(u^a u^b - v^a v^b) e_{ab}^A(\hat{n})$$

$$\text{Cross-Correlation of two detectors I and J : } \langle C(f, t) \rangle = \frac{2}{\tau} \langle \tilde{h}_I(f, t) \tilde{h}_J^*(f, t) \rangle = H(f) \int_{S^2} d^2\theta \gamma(\hat{n}, f, t) \mathcal{P}(\hat{n}, f)$$

$$\gamma(\hat{n}, f, t) = \frac{1}{2} \sum_A F_1^A(\hat{n}, t) F_2^A(\hat{n}, t) e^{i2\pi f \hat{n} \cdot \Delta \vec{x} / c}$$

$\gamma(\hat{n}, f, t)$ : a geometry factor depends the separation of detectors and relative orientation of arms



Ain, Suresh and Mitra 2018

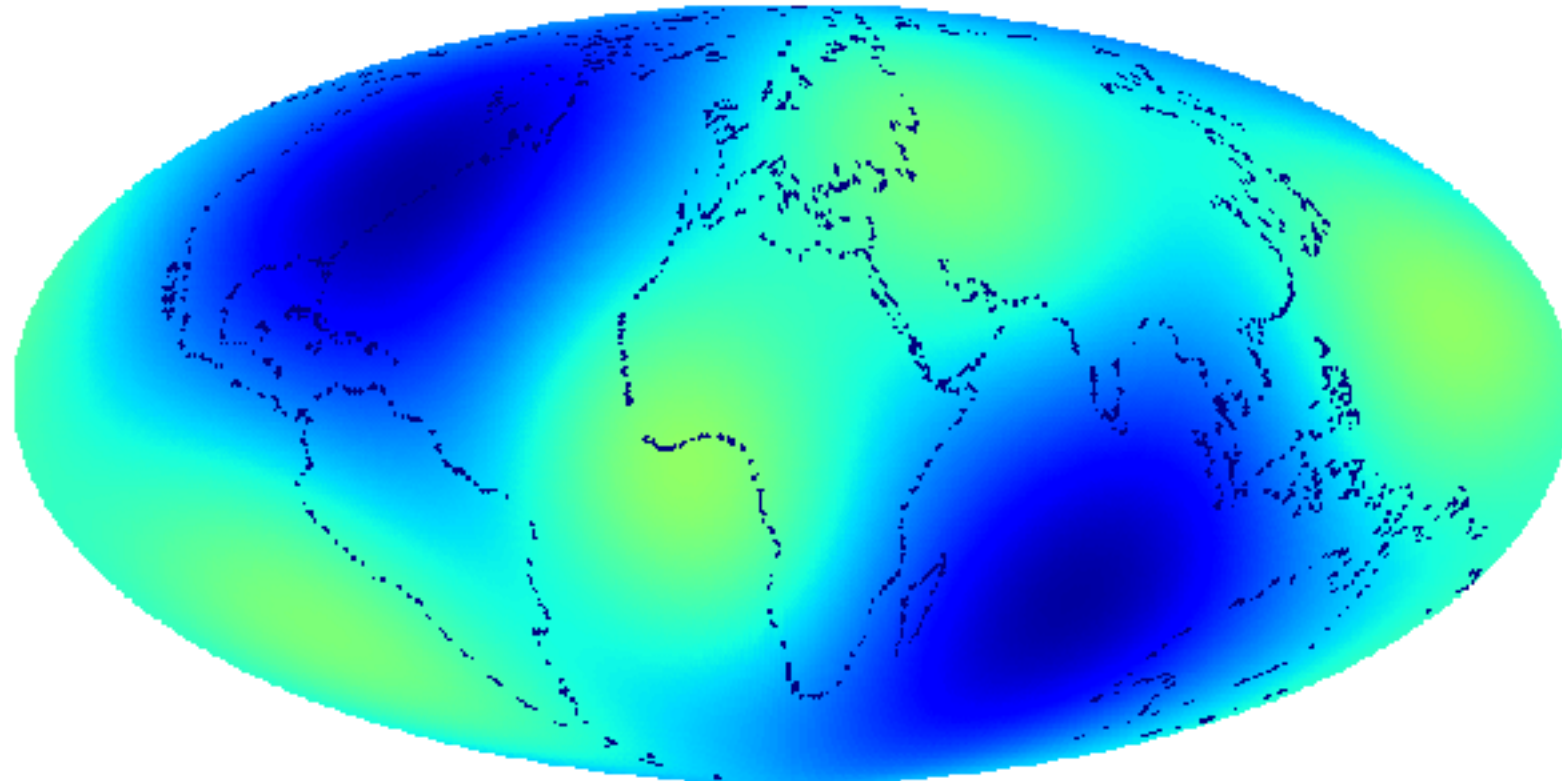


# Geometric factor H1-L1

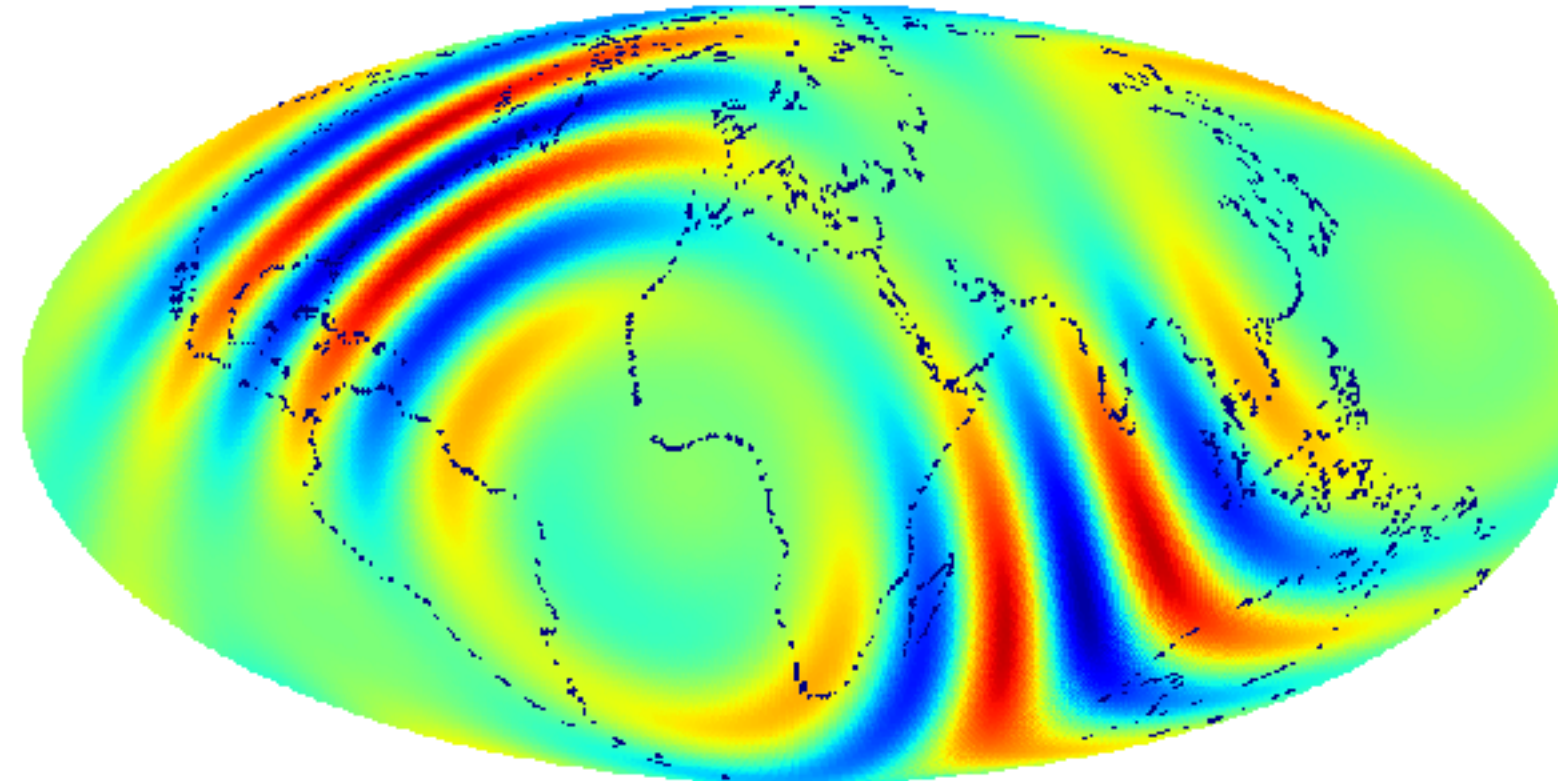
- $\gamma(\hat{n}, f = 0, t)$ , around the vicinity of two detectors, gives the size of field of view
- For higher frequencies, lines indicate regions with the same time delay to two detectors.
- Separation between the positive and negative lobes response provides the resolution of the image.
- The location of the positive and negative lobes are shifted relative to one another for the real and imaginary parts

- $$\Delta\theta \simeq \frac{\text{wavelength}}{2\Delta x}$$

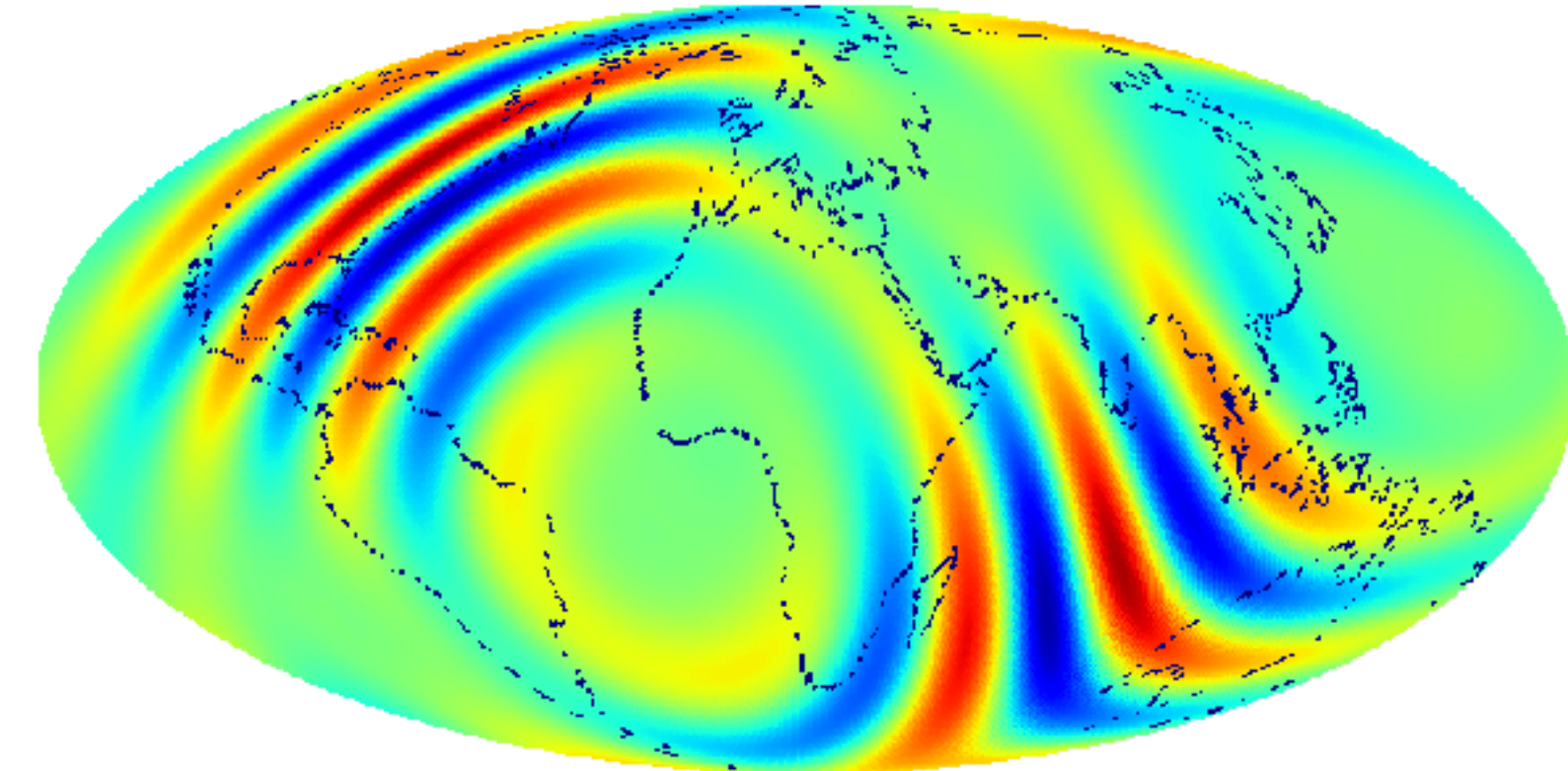
L1-H1, real, f=0Hz



L1-H1, real, f=200Hz



L1-H1, imaginary, f=200Hz



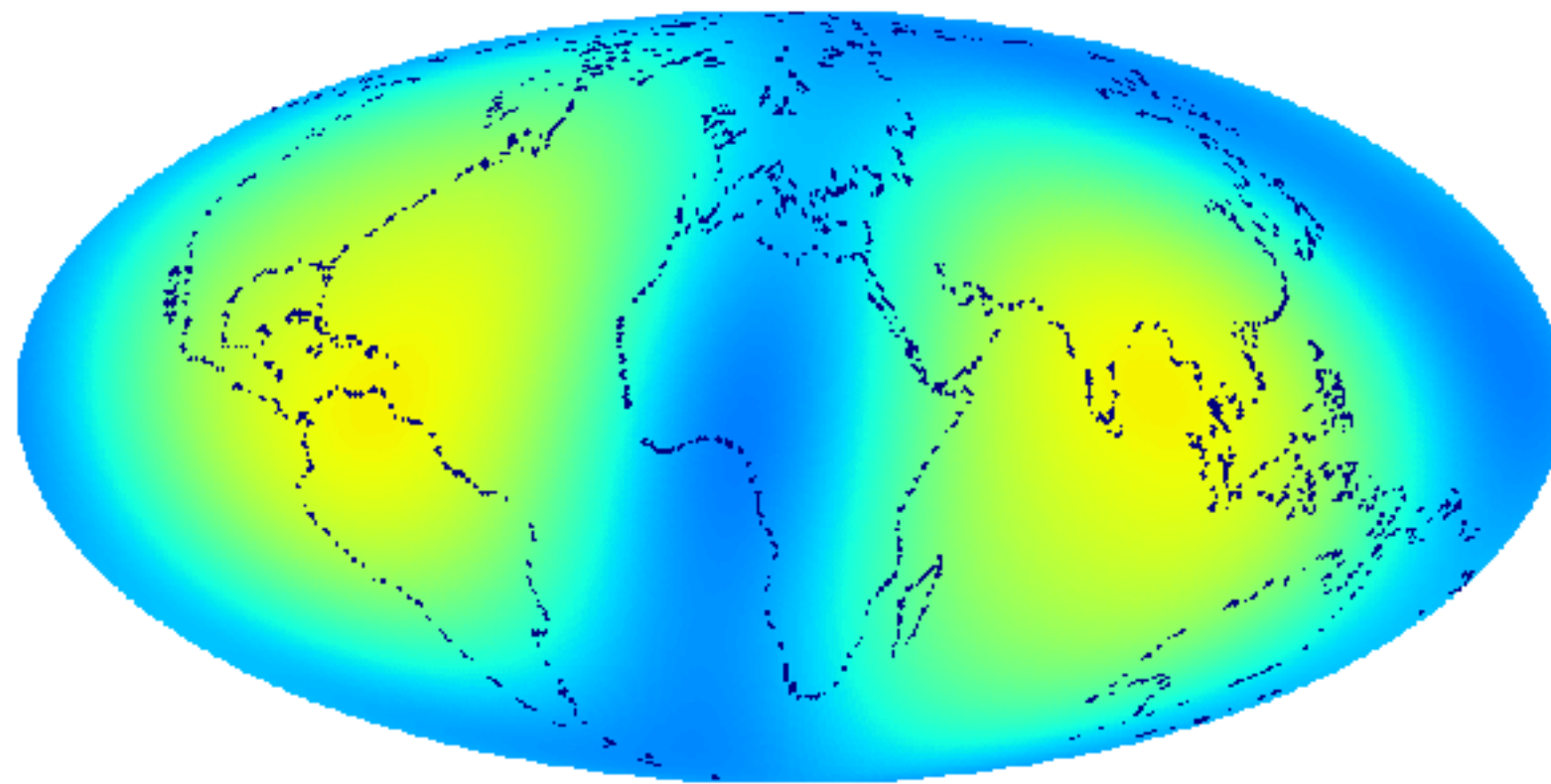


# Geometric factor Virgo-KAGRA

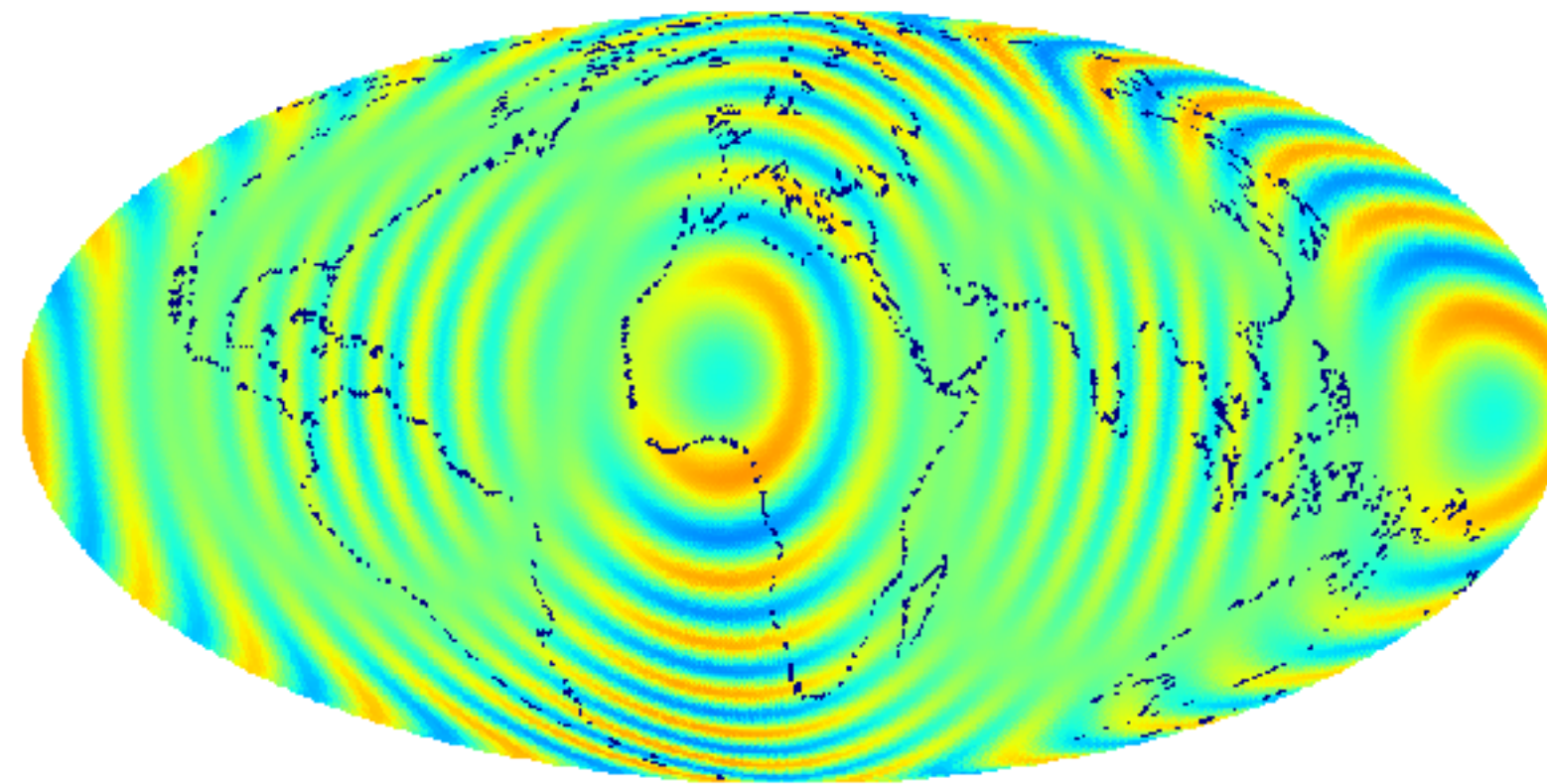
- $\gamma(\hat{n}, f = 0, t)$ , around the vicinity of two detectors, gives the size of field of view
- For higher frequencies, lines indicate regions with the same time delay to two detectors.
- Separation between the positive and negative lobes response provides the resolution of the image.
- The location of the positive and negative lobes are shifted relative to one another for the real and imaginary parts

- $$\Delta\theta \simeq \frac{\text{wavelength}}{2\Delta x}$$

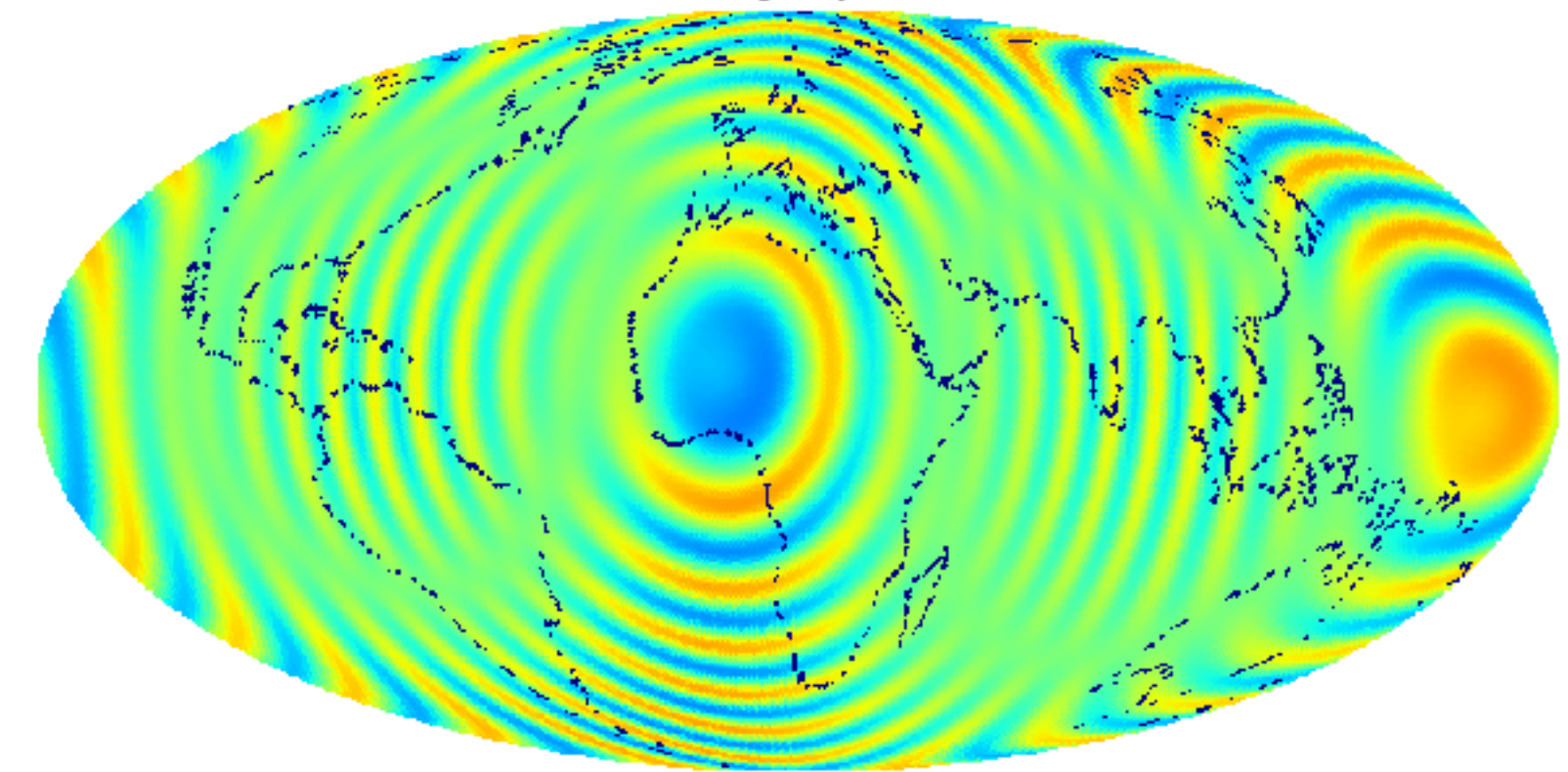
V1-K1, real, f=0Hz



V1-K1, real, f=200Hz



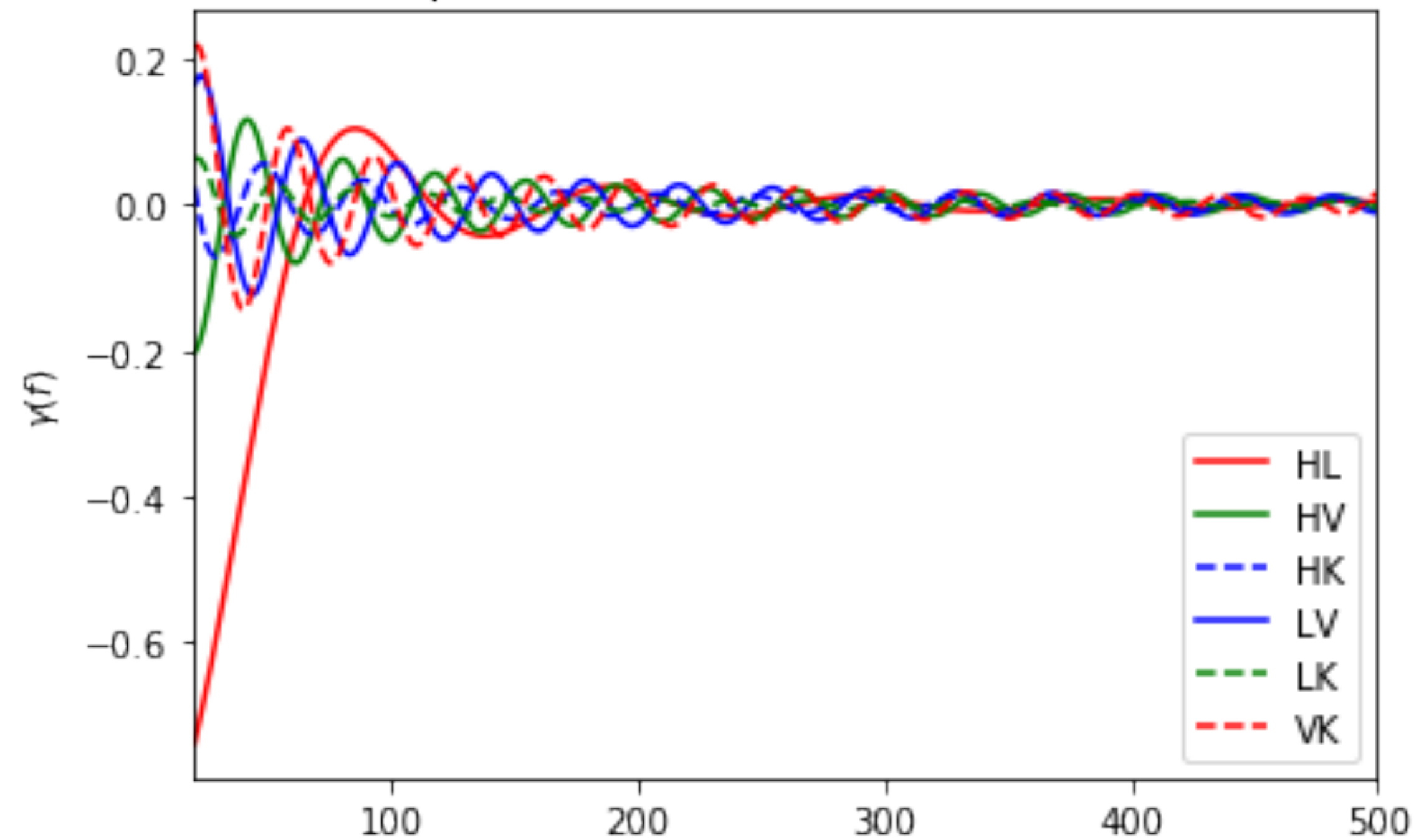
V1-K1, imaginary, f=200Hz



# Isotropic Background

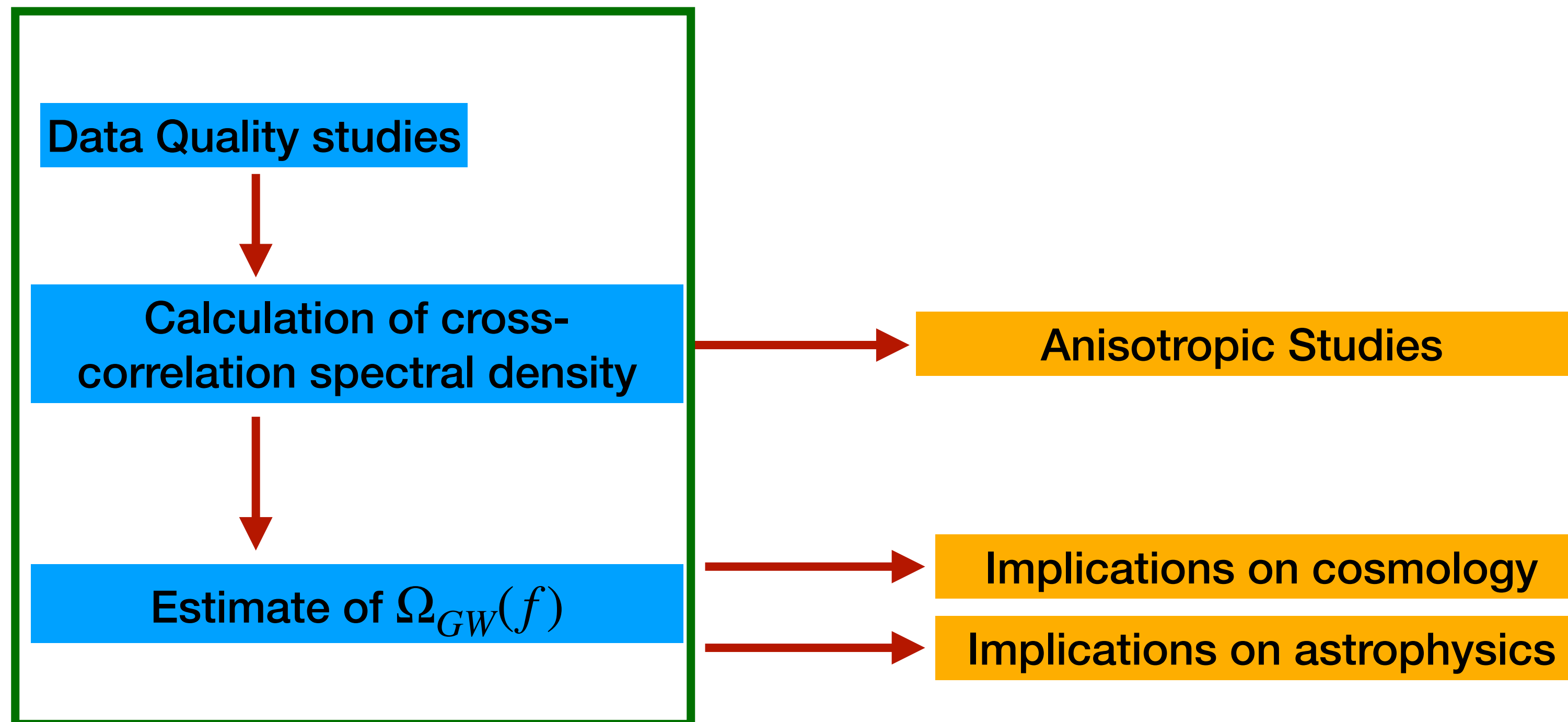
$$\Gamma_{IJ}(f) = \frac{1}{8\pi} \int d^2\Omega_{\hat{n}} \sum_A F_I^A(\hat{\theta}, t) F_J^A(\hat{\theta}, t) e^{i2\pi f \hat{\theta} \cdot \Delta \vec{x} / c}$$

$\Gamma_{IJ}(f)$  is the so-called overlap function of two detectors. It is like the transfer function between GW strain power  $S_h(f)$  and cross power  $\langle C(f, t) \rangle$





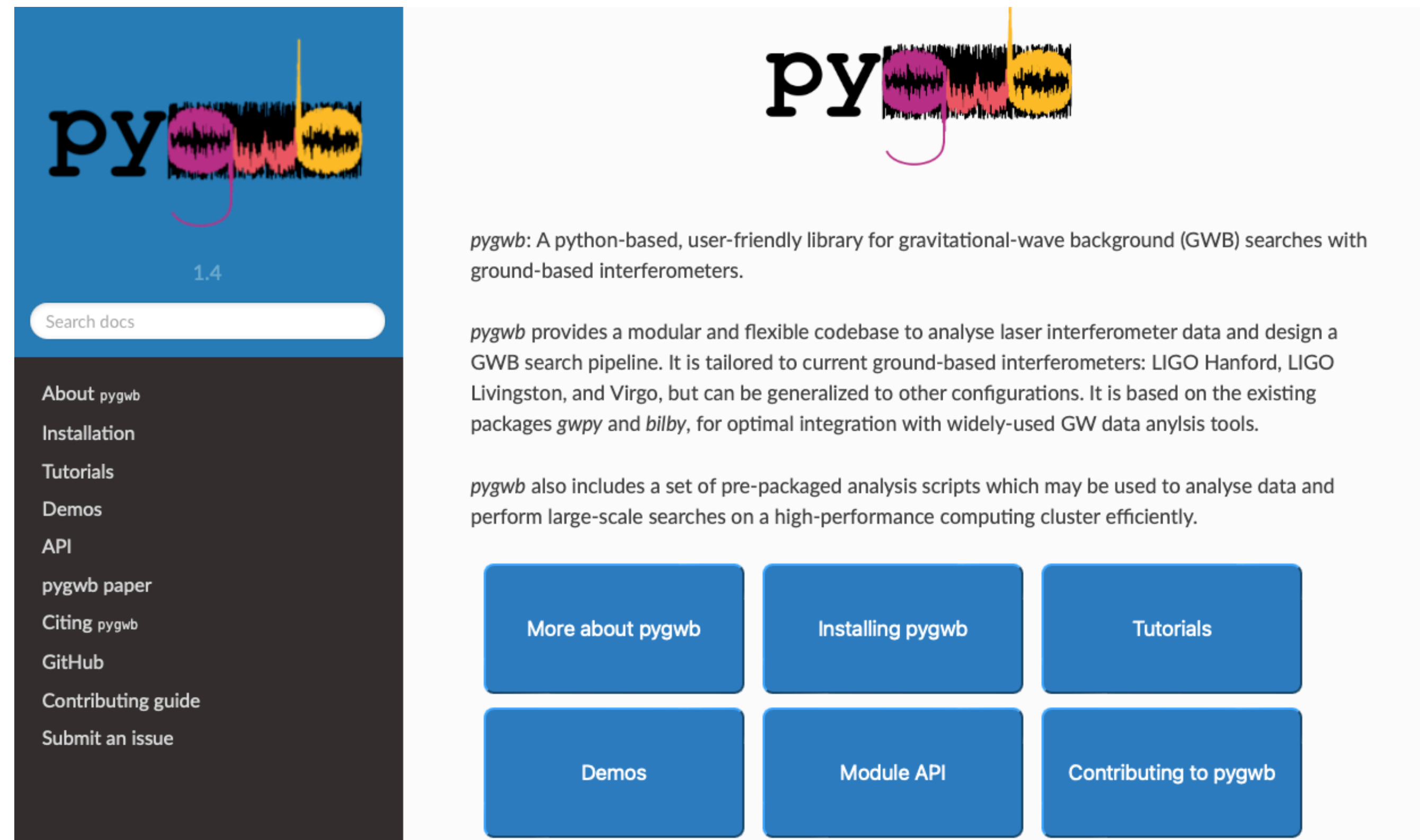
# Analysis Processes



# Pygwb: Isotropic Search pipeline

<https://pygwb.docs.ligo.org/pygwb/>

- Analyzing the data
- Run statistical checks
- Parameter estimation
- Simulate your own data



**pygwb**

1.4

Search docs

About pygwb  
Installation  
Tutorials  
Demos  
API  
pygwb paper  
Citing pygwb  
GitHub  
Contributing guide  
Submit an issue

*pygwb*: A python-based, user-friendly library for gravitational-wave background (GWB) searches with ground-based interferometers.

*pygwb* provides a modular and flexible codebase to analyse laser interferometer data and design a GWB search pipeline. It is tailored to current ground-based interferometers: LIGO Hanford, LIGO Livingston, and Virgo, but can be generalized to other configurations. It is based on the existing packages *gwpy* and *bilby*, for optimal integration with widely-used GW data analysis tools.

*pygwb* also includes a set of pre-packaged analysis scripts which may be used to analyse data and perform large-scale searches on a high-performance computing cluster efficiently.

More about pygwb   Installing pygwb   Tutorials

Demos   Module API   Contributing to pygwb



# Pygwb: Isotropic Search pipeline

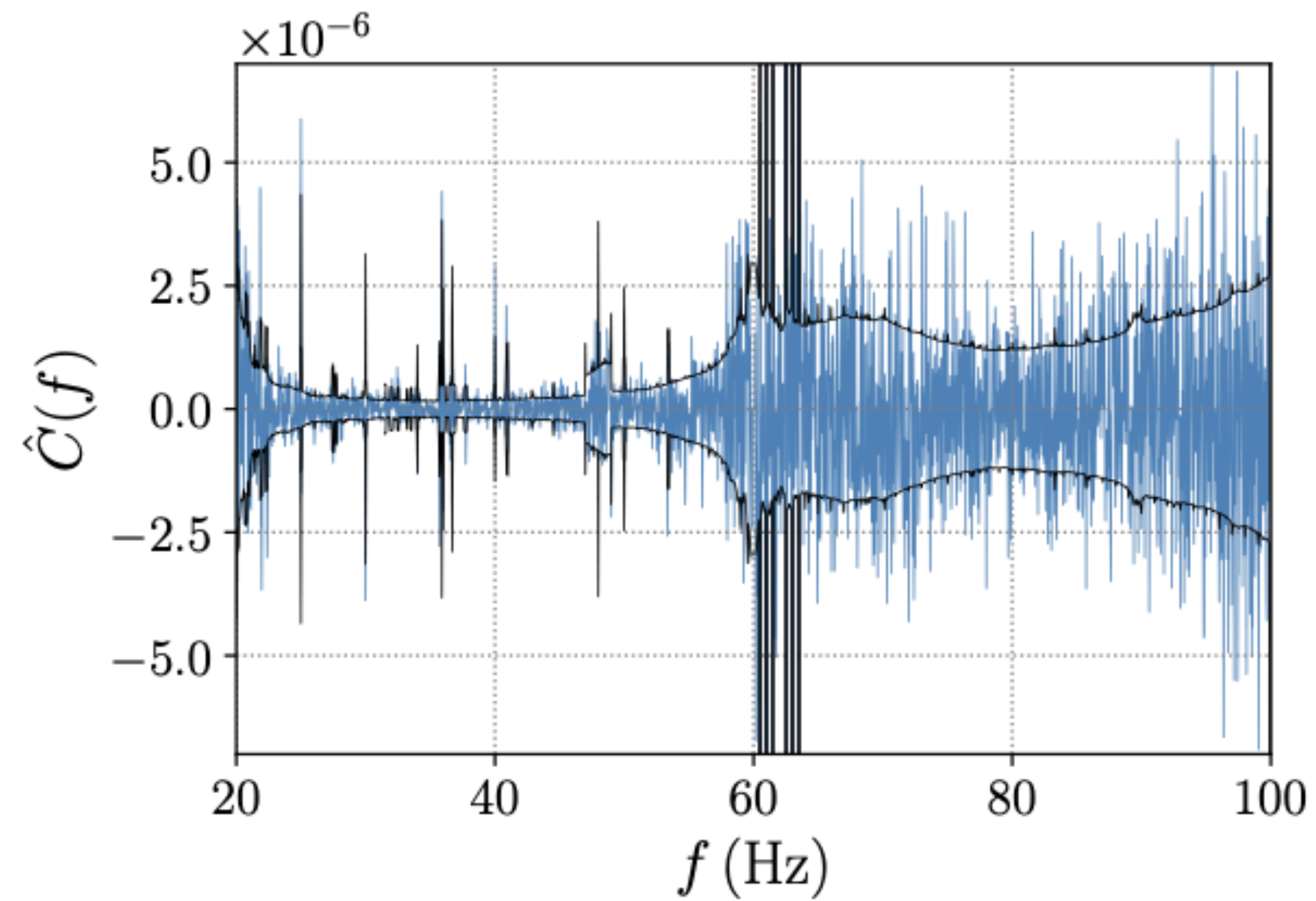
We define an estimator  $\hat{C}_{IJ} = \frac{2 \operatorname{Re}[\tilde{s}_I(f)\tilde{s}_J^*(f)]}{T \Gamma_{IJ}(f)S_0(f)}$ , where  $S_0(f) = \frac{3H_0^2}{10\pi^2 f^3}$  and T is the duration of segment.

$$\text{Uncertainty: } \sigma^2 = \frac{1}{2T\Delta f} \frac{P_I(f)P_J(f)}{\Gamma_{IJ}^2(f)S_0^2(f)}$$

- Analysis parameters:
  - Duration of segments : 192 s
  - Use the Hann window for FFT and Overlap factor is 50%
  - Sampling rate: downsample from 16384 Hz to 4096 Hz
  - Coarse-grain to the frequency resolution 1/32 Hz
  - Analysis frequency: 20-1726Hz
- Removing artifact data:
  - Applying gating scheme to remove loud glitches
  - Delta-sigma cut to remove the non-stationary
  - Notch noise lines due (calibration lines, power line harmonics, etc.)

# O3 Isotropic Results

PRD 104, 022004 (2021)

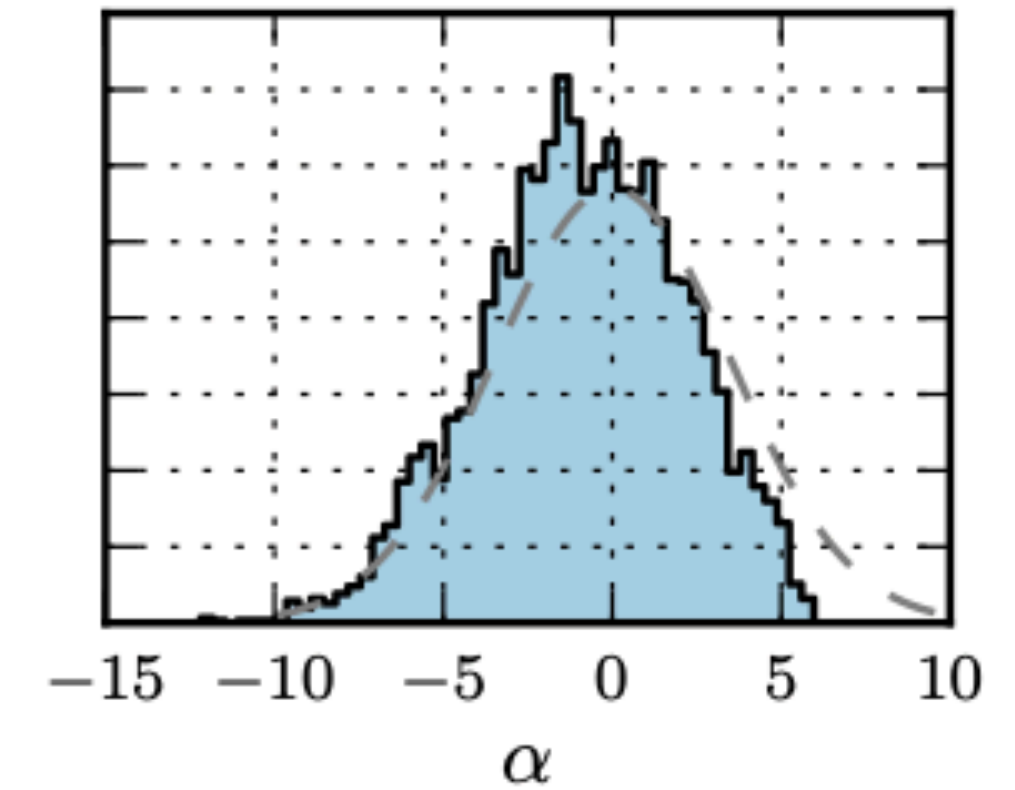
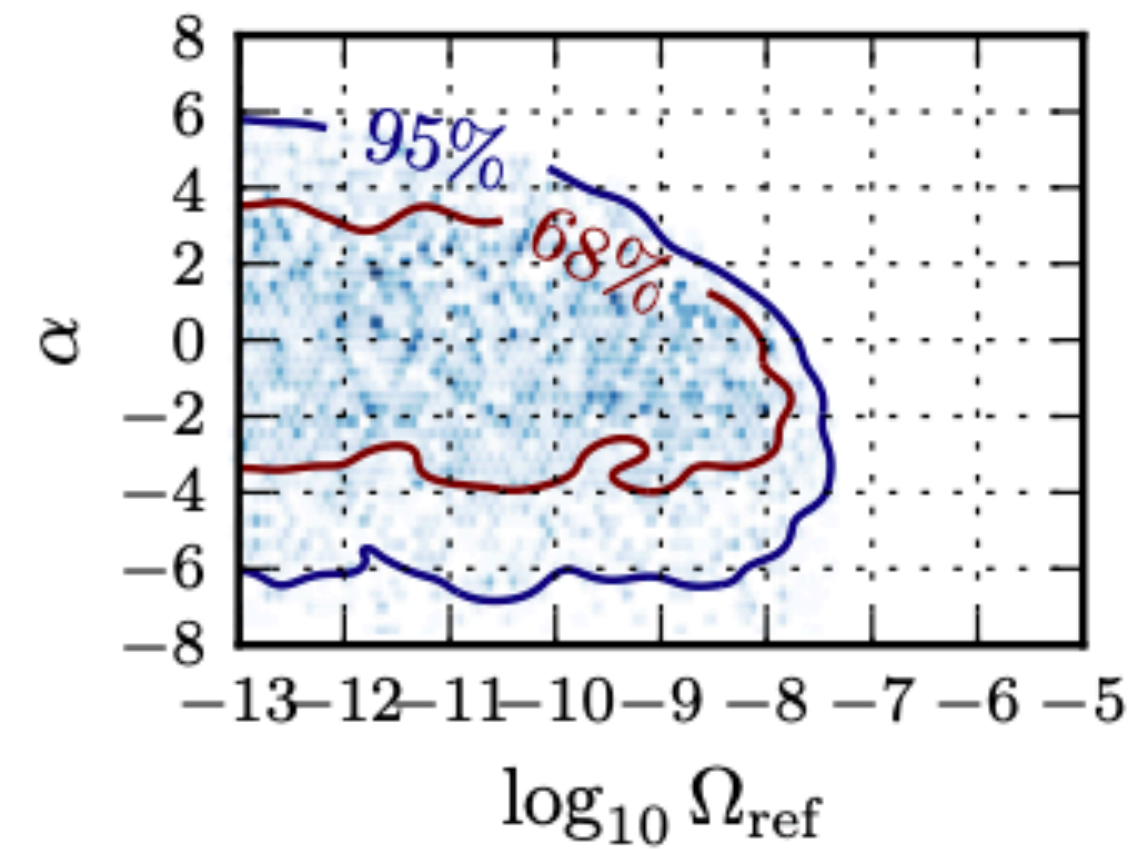
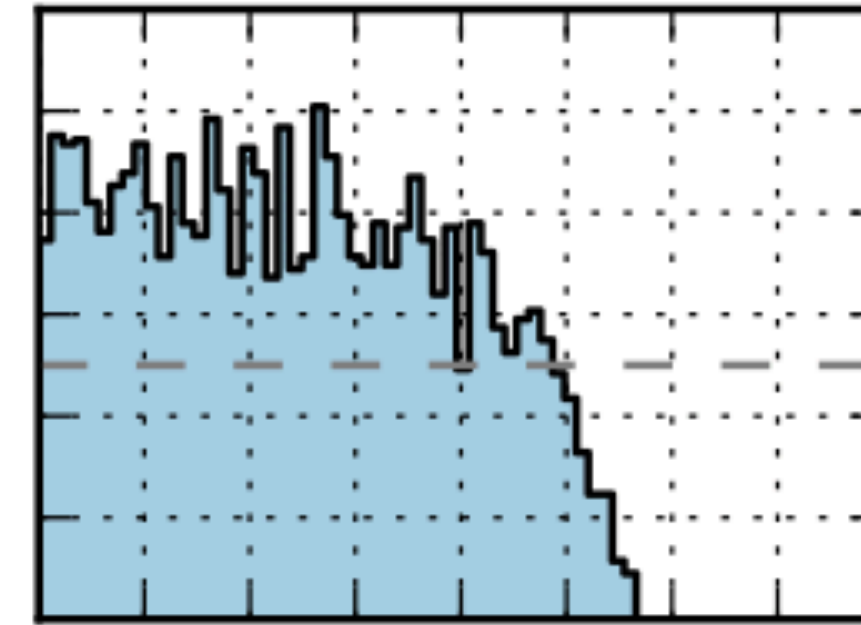


Cross-correlation spectra combining from O1-O3 (including O3 Virgo). The spectrum is consistent with expectations from uncorrelated, Gaussian noise.

# O3 Isotropic Results

Upper limits on  $\Omega_{gw}(f = 25\text{Hz})$

$\alpha$	Uniform prior			Log-uniform prior		
	O3	O2 [43]	Improvement	O3	O2 [43]	Improvement
0	$1.7 \times 10^{-8}$	$6.0 \times 10^{-8}$	3.6	$5.8 \times 10^{-9}$	$3.5 \times 10^{-8}$	6.0
2/3	$1.2 \times 10^{-8}$	$4.8 \times 10^{-8}$	4.0	$3.4 \times 10^{-9}$	$3.0 \times 10^{-8}$	8.8
3	$1.3 \times 10^{-9}$	$7.9 \times 10^{-9}$	5.9	$3.9 \times 10^{-10}$	$5.1 \times 10^{-9}$	13.1
Marg.	$2.7 \times 10^{-8}$	$1.1 \times 10^{-7}$	4.1	$6.6 \times 10^{-9}$	$3.4 \times 10^{-8}$	5.1



# Fiducial models predictions and projected sensitivities

